Encapsulation of Insulin-Secreting Cells Expressing a Genetically Encoded Fluorescent Calcium Indicator for Cell-Based Sensing In Vivo

Christophe Boss, Umberto De Marchi, Aurélie Hermant, Mouna Conrad, Federico Sizzano, Alessio Palini, Andreas Wiederkehr, and Nicolas Bouche*

The development of cell-based biosensors that give insight into cell and tissue function in vivo is an attractive technology for biomedical research. Here, the development of a cell line expressing a fluorescent calcium sensor for the study of beta-cell function in vivo is reported. The bioresponsive cell model is based on INS-1E pancreatic beta-cells, stably expressing the genetically encoded cameleon-based fluorescent sensor YC3.6$_{cyto}$. Following single-cell selection and expansion, functional testing and in vitro encapsulation experiments are used to identify a suitable clone of INS-1E cells expressing the calcium sensor. This clone is transplanted subcutaneous in mouse using a cell macroencapsulation system based on flat sheet porous membranes. Cells in the implanted capsules are able to respond to glucose in vivo by secreting insulin and thereby contributing to the regulation of glycaemia in the mice. Furthermore, fluorescence imaging of explanted devices shows that encapsulated cells maintain high level expression of YC3.6$_{cyto}$ in vivo. In conclusion, these data show that encapsulated INS-1E cells stably expressing a genetically encoded calcium sensor can be successfully implanted in vivo, and therefore serve as biosensing element or in vivo model to longitudinally monitor the function of pancreatic beta-cells.

1. Introduction

Fluorescent sensors and reporter gene technology are widely used to study cell signaling in health and related to the development of chronic diseases such as type 2 diabetes.[1] Bioimaging allows observing dynamic molecular processes in living cells using fluorescence microscopy. Genetically encoded sensors have been developed to follow the dynamics of intracellular parameters such as [Ca^{2+}], [ATP], [Glucose], pH, or the redox state.[2–4] Fluorescence assays have also been applied in vivo to gain information about biological events in the whole organism, since the in vivo microenvironment critically determines many physiological and pathological processes.[5] However, in vivo imaging relies on external and highly sensitive detectors, which have intrinsic limitations such as tissue absorption, light scattering or tissue autofluorescence.[6] Also, such whole-body imaging instruments do not allow continuous monitoring and require a lot of animal handling.

An alternative to external imaging would be to record fluorescent signals with an implanted ultrasmall optical detector. Such an implantable cell-based biosensor would allow many preclinical research applications by taking advantage of the wide variety of available genetic probes. In particular in the context of metabolic health research, this technology would allow the continuous recording of cellular mechanisms in vivo under specific conditions such as changes in diet, exercise or aging. On a long term basis, such devices may pave the way for implantable diagnostic systems to monitor health status. Cells are indeed natural sensors in the body. Their use in implantable devices may allow long-term applications in vivo, a major problem encountered when using other biosensing technologies.[7] The development of fully implantable cell-based biosensors is made possible by the combination of long term implantation using cell encapsulation technology,[8,9] the genetic engineering of optically responsive cell lines and the recent development in ultrasmall optics and implantable systems.[10,11]

Monitoring cytosolic Ca^{2+} dynamics in vivo is of particular interest, since Ca^{2+} is an extremely versatile intracellular messenger linked to cell activation in a wide range of biological processes.[12] Spatial/temporal control of intracellular Ca^{2+} signaling plays a key role in physiology and pathology. For example, nutrient-sensing in pancreatic beta-cells is associated with calcium rises in both the cytosol and mitochondria.[13] The development of a cell-based biosensor measuring intracellular

Dr. C. Boss, M. Conrad, N. Bouche
Device Engineering
Nestlé Institute of Health Sciences
EPFL Innovation Park, 1015 Lausanne, Switzerland
E-mail: christophe.boss@rd.nestle.com
Dr. U. De Marchi, A. Hermant, Dr. A. Wiederkehr
Mitochondrial Function
Nestlé Institute of Health Sciences
EPFL Innovation Park, 1015 Lausanne, Switzerland
Dr. F. Sizzano, Dr. A. Palini
Flow Cytometry
Nestlé Institute of Health Sciences
EPFL Innovation Park, 1015 Lausanne, Switzerland

DOI: 10.1002/adhm.201600869

calcium in pancreatic beta-cells would allow to follow beta-cell activation in vivo. Nutrient stimulated Ca^{2+}-signaling in beta-cells and its relationship to diet, exercise, and aging could be studied "in situ".

Intracellular calcium can be measured using genetically encoded cameleon-based fluorescent sensors, which are FRET (fluorescence resonance energy transfer) -based ratiometric indicators optimized to sense calcium without interfering with the function of endogenous proteins.[2,14] The probes consist of a cyan and a yellow fluorescent protein linked by a Ca^{2+}-sensing module. Binding of Ca^{2+} to this module brings the two fluorescent moieties in closer proximity, favoring fluorescence resonance energy transfer and causing a shift in fluorescence emission from cyan to yellow. The Cameleons have several advantages over other calcium sensing probes. Cameleon sensors are characterized by expanded dynamics, reduced interference from endogenous proteins and they do not depend on other cofactors but calcium for changes in their emission spectrum.[15,16] The Cameleons bind calcium reversibly allowing to continuously follow changes in intracellular calcium concentrations. These genetic probes when stably expressed will be continuously produced by the cell for long-term sensing of calcium such as required for in vivo experiments.[15] The Cameleons can also be targeted for specific measurements in subcellular compartments.[17] Depending on the cell lines developed, the proposed biosensor approach could also be extended to measure Ca^{2+} in different cell types. In addition, other cameleon-based fluorescent sensors could be used to follow additional intracellular parameters.[3]

Beside the development of the optical sensor, the essential building block of the proposed cell-based biosensor is the development of a suitable bioresponsive cell model. Here, we present the development of a beta-cell line stably expressing a cameleon-based calcium sensor. We describe the method to create INS-1E cell aggregates essential for subsequent successful encapsulation in vitro. Next, INS-1E clones expressing the calcium sensor $YC3.6_{cyto}$ (INS-1E-$YC3.6_{cyto}$) were generated and characterized in vitro, including clone stability, calcium sensor function, and encapsulation capabilities. Finally implantation in mice was used to show that encapsulated INS-1E-$YC3.6_{cyto}$ cells survived and were functional in vivo for extended periods of time and can therefore be used as model to longitudinally monitor the function of insulin-secreting cells in vivo.

2. Results

2.1. INS-1E Cell Aggregation and Encapsulation

In macroencapsulation systems where the membrane acts as a barrier which isolates encapsulated cells from the host, it is essential to provide the cells with a scaffold which will support their expansion and 3D colonization of the device inner space.[8] A variety of matrices have been used such as collagen or laminin containing hydrogels and natural extracellular matrixes.[9] Cell aggregation is an alternative method to provide a microenvironment that favors cell–cell interaction and mimics the in vivo environment. Cell aggregation has the advantage of avoiding any diffusion of matrix compounds, which could influence the host reaction or biocompatibility to the implanted device.[9] Previously, encapsulation of cell aggregates has been successfully used for the terminal in vivo differentiation of pancreatic beta-cell derived from human embryonic stem cells.[18] Cell aggregates mimic cell–cell communication and islet structure, which is known to be essential for the proper function of pancreatic beta-cells.[19] In addition, good glucose-stimulated insulin secretion was reported for INS-1E aggregates, prompting us to study encapsulation of INS-1E cell aggregates.[20] We needed to develop a robust process forming INS-1E aggregates of reproducible size and shape. The typical size of an islet of Langerhans lies between 100 and 200 µm, which was a good target for the aggregate size.[21] Cell suspensions were placed in ultralow attachment 6-well culture plates on an orbital shaker. To determine optimal parameters for aggregate formation, we tested the effect of cell concentration, shaking rotation speed and time in suspension culture on aggregate formation. Changing the rotation speed from 85, 95 to 105 rpm had a noticeable effect on aggregate size after 1 d in suspension culture (**Figure 1**A). Small aggregates were obtained at 85 rpm and the aggregate size increased with the rotation speed. At 105 rpm we noticed increased aggregate size heterogeneity. The cell concentration influenced the aggregate size to a lesser degree (Figure 1B). Larger aggregates were observed at low cell concentrations (1 million per well). Increased heterogeneity in aggregate size was observed at the highest cell density (5 million cells per well). The time in suspension culture was another parameter to control for aggregate size. The aggregates progressively grew with time in suspension culture (Figure 1C,D).

Cellular health was further studied in aggregates started at 2.5 million cells per well at a speed of 95 rpm for 1 d. Cells were stained with the live cell-stain fluorescent marker calcein AM. Dead cells were identified in the same samples with ethidium homodimer-1 which permeates cells with compromised plasma membranes. Only a very small fraction of the INS-1E cells were ethidium homodimer-1 positive, showing that INS-1E cells are healthy when cultured under our optimized aggregation conditions (Figure 1E). Subsequent experiments were performed with 2.5 million cells per well in 6-well plates and the cells were allowed to aggregate at a rotation speed of 95 rpm for 1 d.

To investigate the feasibility of INS-1E cell encapsulation, we loaded capsules with a volume of 30 µL of INS-1E cell aggregates, representing ≈3 million cells. Encapsulated cells were cultured for five weeks in vitro and functionality of the cells was assessed by measuring glucose-induced insulin secretion (Figure 1F). At all time-points between 2 and 35 d in culture, INS-1E cells maintained their ability to respond to glucose, raising insulin secretion by more than threefold (Figure 1F inset). The amounts of both basal and stimulated insulin secretion from INS-1E cells reduced significantly between 2 and 7 d of culture in the capsules but glucose responsiveness was maintained (Figure 1F). Stirring of the medium containing the encapsulated INS-1E cell aggregates may be important partly by enhancing oxygen and nutrients supply. We therefore compared encapsulated cells cultured in stirred and unstirred medium. Consistently with the higher cell growth inside the capsule in stirred medium, capsules in stirred medium also showed three to four times higher insulin secretion after four weeks in culture (Figure 1G,H). These results demonstrate that INS-1E cells

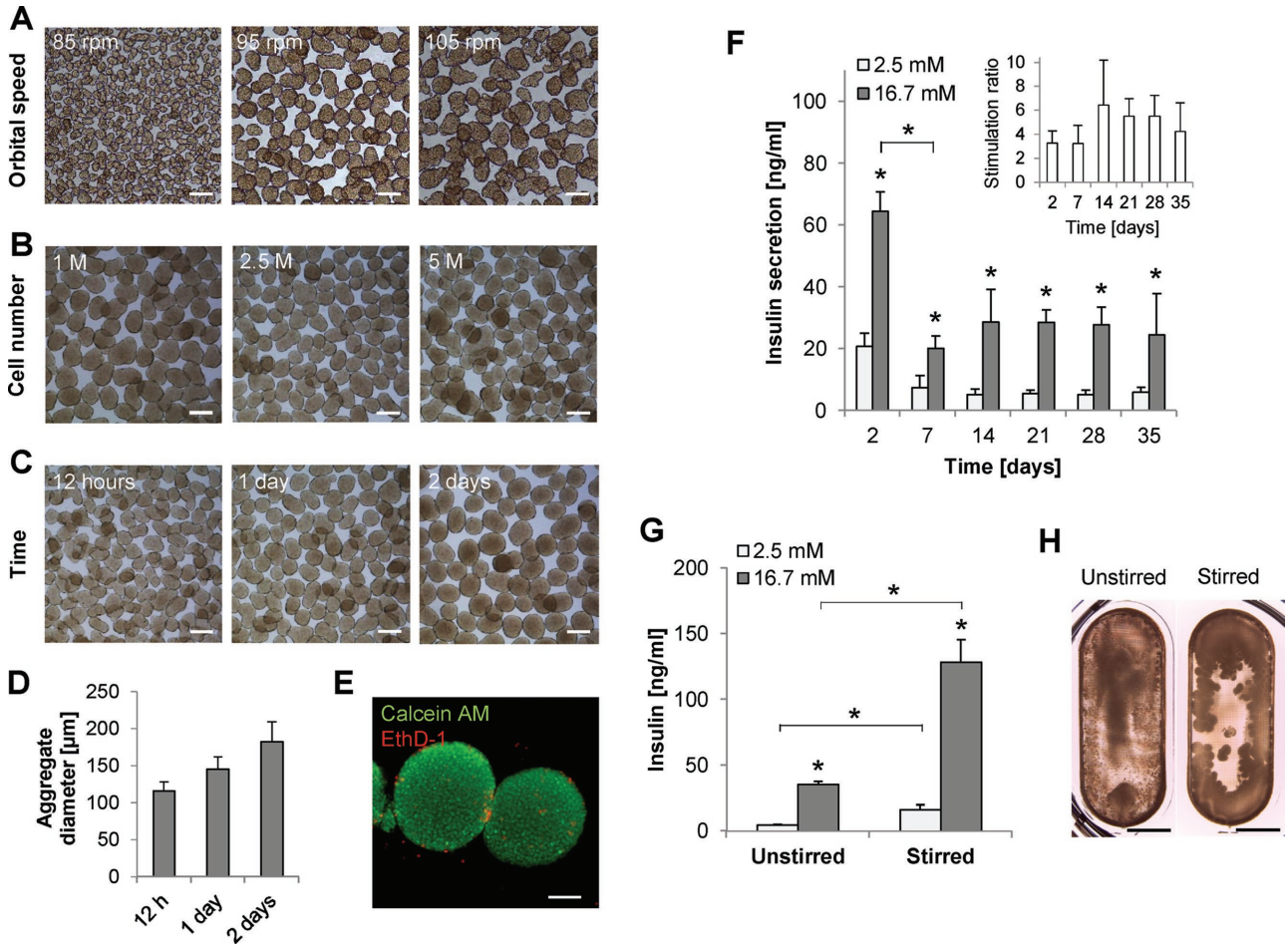

Figure 1. Aggregation and in vitro encapsulation of INS-1E cells. A) Aggregates formed using various orbital speeds: 85, 95, and 105 rpm. Initial cell number: 2.5 million cells per well, aggregation time: 1 d. Scale bars: 200 µm. B) Aggregates formed using various cell numbers: 1, 2.5, and 5 million cells per well. Orbital speed: 95 rpm, aggregation time: 1 d. Scale bars: 200 µm. C,D) Evolution of aggregate size with time in suspension culture. Orbital speed: 95 rpm, initial cell number: 2.5 million cells per well. Scale bars: 200 µm. Data are expressed as mean ± SD from 40 measurements. E) Fluorescence microscopy of INS-1E cell aggregates stained with live cell-staining (calcein AM, green) and dead cell nuclei-staining dyes (ethidium homodimer-1, red). Orbital speed: 95 rpm, initial cell number: 2.5 million cells per well, aggregation time: 1 d. Scale bar: 100 µm. F) Static glucose-stimulated insulin secretion from encapsulated INS-1E cells cultured in vitro at different time points. Inset: stimulated to basal insulin secretion ratios. Data are expressed as mean ± SD, $N = 5$. Student's t-test: $^*p < 0.05$. G) Comparison of insulin secretion from encapsulated INS-1E cells in stirred and unstirred medium after four weeks in culture. Data are expressed as mean ± SD, $N = 3$. Student's t-test: $^*p < 0.05$. H) Pictures of encapsulation devices showing cell growth in stirred and unstirred medium conditions after 35 d in culture. Scale bars: 5 mm.

can be cultured in a macroencapsulation system, using aggregates as an effective 3D microenvironment favoring cell growth and maintain glucose-induced secretory function. Furthermore, encapsulated INS-1E cells dynamically adapt to the oxygen and nutrient availability.

2.2. Stable INS-1E-YC3.6$_{cyto}$ Clone Generation and Characterization

To continuously monitor Ca^{2+} dynamics in INS-1E pancreatic beta-cells in vivo, we generated clonal cell lines stably expressing the YC3.6$_{cyto}$ calcium sensor. Following transfection with the plasmid, highly fluorescent cells were selected by fluorescence-activated cell sorting (FACS) and cultured for 20 d in selection medium (**Figure 2**A). A second FACS sorting was performed and highly fluorescent single cells were cloned by placing them individually in 96-well plates. Out of 24 positive clones, 3 clones were selected for further characterization, based on fluorescence level, morphology and growth criteria (Figure 2B). Clones 1 and 2 showed canonical morphology and, respectively, high and lower fluorescence levels, whereas clone 3 was highly fluorescent and spontaneously formed small cell clusters in culture, which may be a desired property for later cell aggregation and encapsulation. To test for their stability, the three clones were cultured for nine weeks in absence of selective antibiotics (Figure 2C). Clones 2 and 3 showed good stability, with most of the cells being fluorescent after nine weeks in culture. Only a small fraction of clone 1 cells remained strongly fluorescent. Single cell time-laps microscopy in the three clones demonstrated intact signal transduction following stimulation with glucose. Large cytosolic calcium transients were measured when

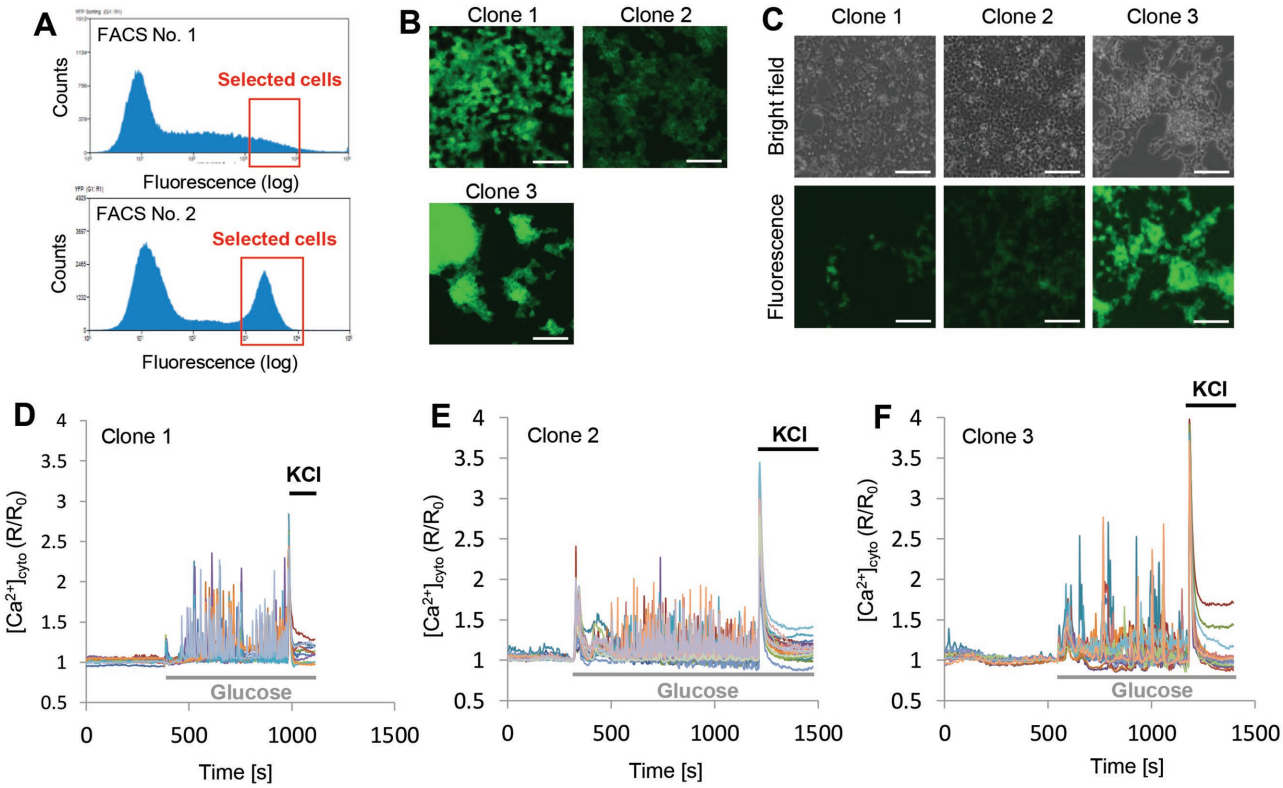

Figure 2. Generation and signal transduction characterization of three INS-1E clonal cell lines expressing the YC3.6$_{cyto}$ calcium sensor. A) Two sequential fluorescence sorting at 488 nm were performed to select positive clones, which were grown up from single-cell. B) Fluorescence pictures of the three clones selected to be extensively tested in vitro, based on fluorescence level, morphology, and growth criteria. Scale bars: 100 µm. C) Fluorescence pictures of the three clones cultured for nine weeks in absence of selective antibiotics. Scale bars: 100 µm. D–F) Single-cell response of the three selected clones of INS-1E-YC3.6$_{cyto}$ cells. Cells were washed with KRBH buffer and sequentially stimulated with glucose (16.7×10^{-3} M) and KCl (30×10^{-3} M). The ratiometric signal (R) was normalized to basal (R_0).

following the fluorescence emission ration at 535/480 nm of the YC3.6$_{cyto}$ calcium sensor excited at 430 nm (Figure 2D–F). In addition, opening of plasma membrane Ca^{2+} channels after depolarization of the plasma membrane with KCl promoted a large increase of the YC3.6$_{cyto}$ ratiometric emission signal.

2.3. In Vitro Evaluation of Clones Encapsulation

To determine which clone would be suitable to be implanted in vivo, we evaluated the aggregation and encapsulation capabilities and the fluorescent properties of the three clones. First, we demonstrated the ability of the three clones to form aggregates, using the suspension culture method (**Figure 3**A). Interestingly, the three clones formed aggregates of different sizes under the same culture conditions. Clones 1 and 2 showed behavior close to native INS-1E cells, whereas larger clusters and more heterogeneity in size was observed for clone 3. The encapsulation of the three clones was assessed by loading 10 µL of aggregates representing ≈1 million cells in 12 devices (Figure 3B). A lower number of cells were used for these experiments as a significant reduction of glucose-induced insulin secretion was observed when loading 3 million cells (Figure 1F). Encapsulated clones were cultured in vitro for 38 d and fluorescence microscopy was used to longitudinally monitor the YC3.6$_{cyto}$ signal of the cells (Figure 3C,D). The fluorescence of the three clones decreased quite rapidly during the first days following cell loading. Clone 3 was least affected as some YC3.6$_{cyto}$ fluorescence was measured throughout the experiment. After 30 d of encapsulation, fluorescence reached close to background levels for clones 1 and 2. This decrease may be due to limited oxygen and nutrient supply and associated cellular stress and a failure to maintain transgene expression. Starting at 30 d, we therefore stirred the medium as an attempt to favor proper supply. This generated a significant increase in the fluorescence signal of clones 1 and 2 and a huge increase in the case of clone 3 (Figure 3D). To test whether stirring the medium was indeed beneficial to maintain cellular health and expression of the fluorescent calcium sensor, we repeated these experiments continuously stirring the medium (Figure 3F). Under these conditions YC3.6 fluorescence increased initially and then remained elevated for the 28 d of the experiment. In control unstirred capsules, fluorescence decreased initially and remained low consistent with our earlier observations (compare Figure 3D,F). At day 19, stirring was initiated in these capsules resulting in a rapid rise in fluorescence of the calcium probe. After a few days, fluorescence reached values as observed in the continuously stirred capsules (Figure 3F). Our results demonstrate that stirring the medium in vitro is an important factor for a protocol aimed to maintain good transgene expression.

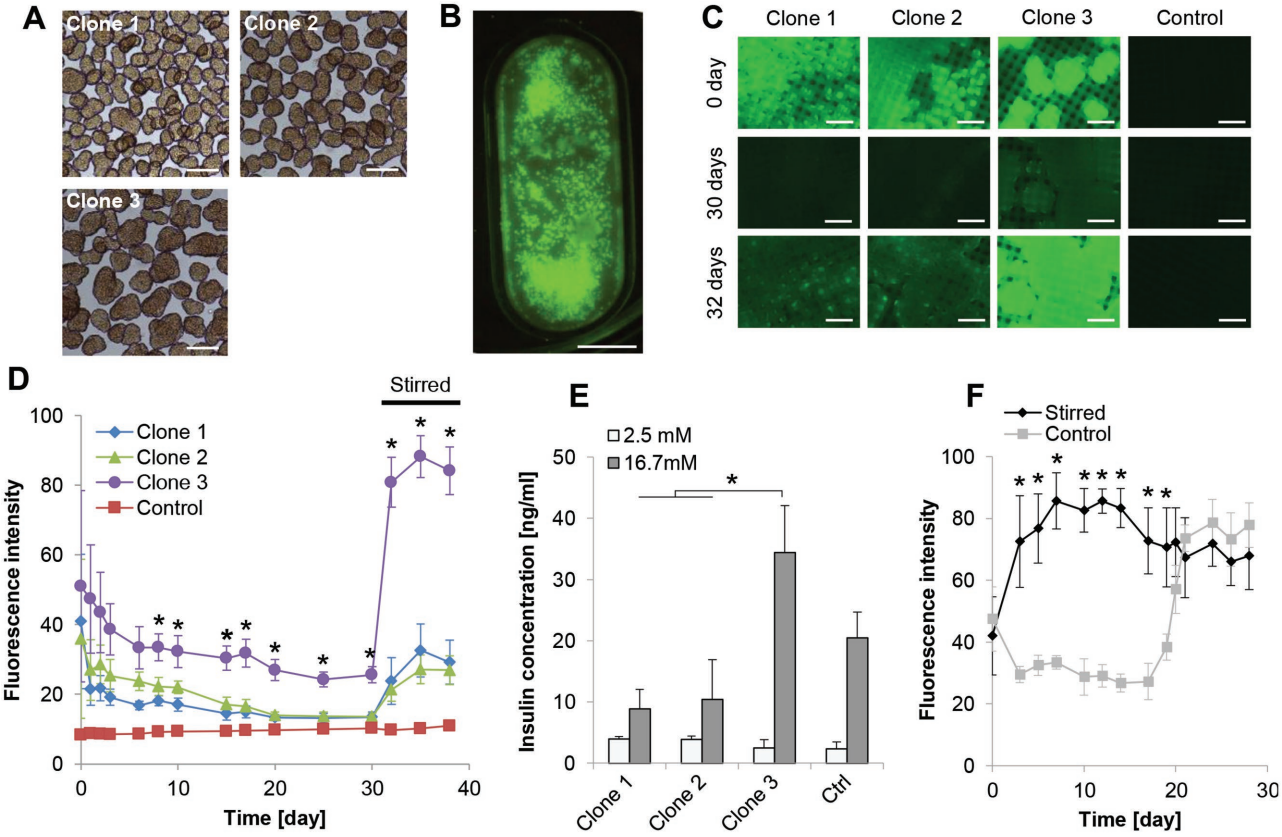

Figure 3. Fluorescence properties and insulin secretion of encapsulated INS-1E-YC3.6$_{cyto}$ clonal cell lines in vitro. A) Pictures of aggregates formed by the three clones after 1 d in suspension culture (2.5 million cells per well, 95 rpm). Scale bars: 200 µm. B) Fluorescence picture of the encapsulation device containing INS-1E-YC3.6$_{cyto}$ clone aggregates. Scale bar: 5 mm. C) Fluorescence pictures of the three selected INS-1E-YC3.6$_{cyto}$ clones and INS-1E control cells in the encapsulation device after 0, 30, and 32 d. Culture conditions were changed from unstirred to stirred medium at day 30. Stirred medium: 95 rpm. Scale bars: 500 µm. D) Evolution of the mean fluorescence intensity for the three clones and INS-1E control cells throughout the in vitro encapsulation experiment. Data are expressed as mean ± SD from nine measurements ($N = 3$). Student's t-test: $^*p < 0.05$. E) Static glucose-induced insulin secretion for the three clones and INS-1E control cells after 30 d in the encapsulation device. Data are expressed as mean ± SD, $N = 3$. Student's t-test: $^*p < 0.05$. F) Fluorescence intensity of clone 3 cultured in stirred medium throughout the experiment. Control: clone 3 cultured in unstirred medium from 0 to 19 d and stirred medium from 19 to 28 d. Stirred medium: 95 rpm. Data are expressed as mean ± SD from nine measurements ($N = 3$). Student's t-test: $^*p < 0.05$.

Fluorescence microscopy also revealed an increase of biomass with time, suggesting an excellent viability of clone 3 in the encapsulation system (Figure 3C). Consistently, at 30 d glucose-induced insulin secretion was much stronger for clone 3 compared to clone 1, clone 2, and even control INS-1E cells (Figure 3E). In addition, clone 3 maintained YC3.6 expression even when cultured in standard medium, in absence of selective antibiotics. These results indicate that clone 3, which displays particularly robust glucose-induced insulin secretion even after culture inside the capsule, may be a good cellular model to monitor cytosolic Ca^{2+} dynamics in vivo.

2.4. Viability and Function of Encapsulated Cells In Vivo

The in vitro results on clone 3 prompted us to investigate whether encapsulated INS-1E-YC3.6$_{cyto}$ aggregates retained function following implantation in mice. Since initial cell density may be a critical factor for the successful expansion of the cells within the encapsulation device, we tested two initial cell densities. With a high cell number, the limited oxygen and nutrient supply within the capsule may cause a massive cell death generating necrotic cells inside the capsule, whereas a too small cell population may not survive the first critical weeks following implantation with low cell number.[8] Nine devices containing 1 million cells and nine devices containing 3 million cells were implanted in the dorsal subcutaneous space of immune-compromised SCID/beige mice. In addition, two mice without implants were used as control. Survival and function of encapsulated and implanted INS-1E-YC3.6$_{cyto}$ cells was evaluated at two, four, and eight weeks postimplantation using glucose tolerance tests. Glucose-induced insulin secretion from implanted INS-1E cells should accelerate the lowering of plasma glucose levels during a glucose tolerance test.

Two weeks postimplantation, glucose was cleared more rapidly in a few mice, mainly those implanted with capsules containing 3 million cells (**Figure 4**A). Faster glucose clearance was observed for 16 out of 18 implanted mice four weeks after implantation. The two exceptions had been implanted with devices loaded initially with 1 million cells (Figure 4B).

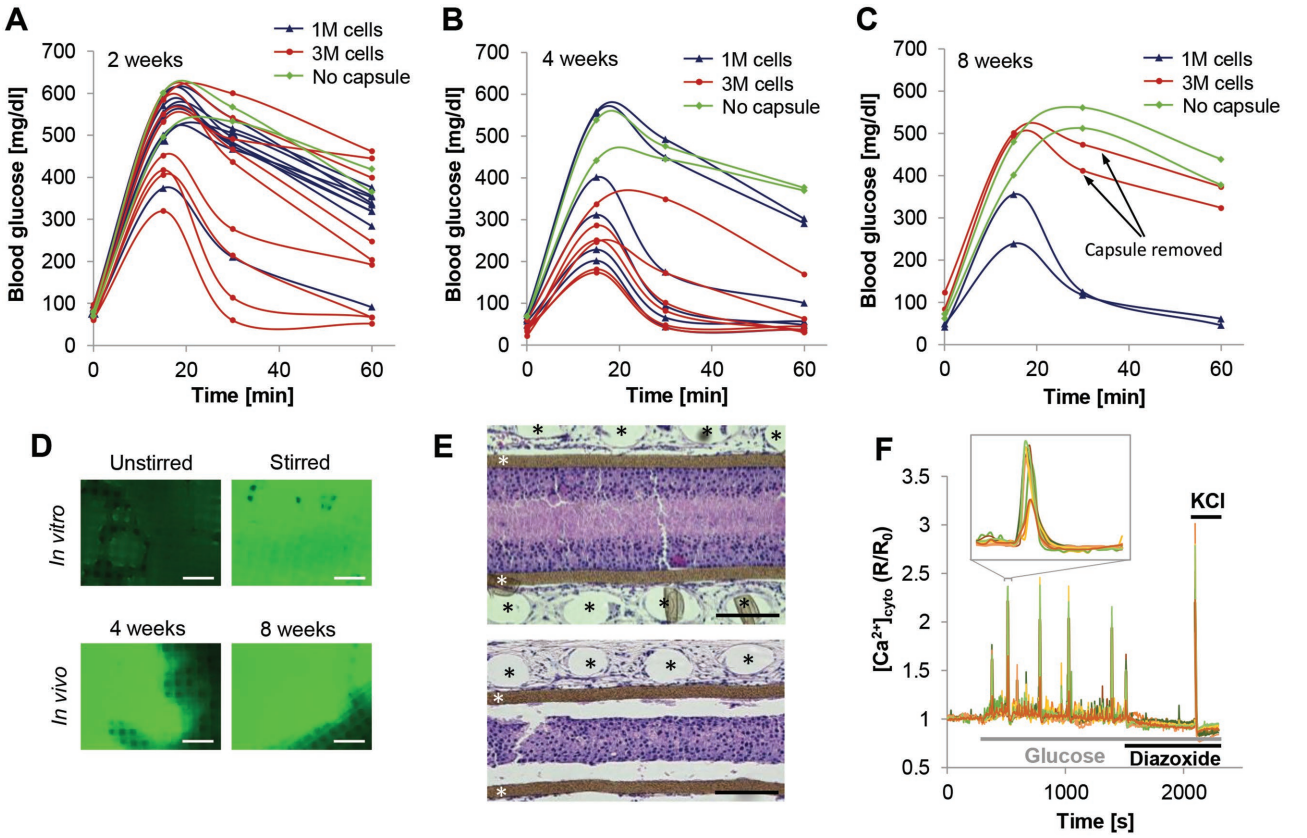

Figure 4. In vivo characterization of blood glucose level, fluorescence properties and signal transduction of encapsulated INS-1E-YC3.6$_{cyto}$ cells. A,B) Blood glucose levels of individual mice following intraperitoneal glucose administration two weeks (A) and four weeks (B) postimplantation. C) Blood glucose levels in response to glucose tolerance test eight weeks postimplantation. Capsules from the 3 million cells condition were surgically removed one week before. D) Fluorescence pictures of encapsulated cells in vivo immediately after taken out of mice at four weeks and eight weeks following implantation, in comparison with capsules cultured in vitro in unstirred and stirred conditions. Scale bars: 500 µm. E) Photomicrographs of histological sections across encapsulation devices eight weeks postimplantation, stained with hematoxylin and eosin. White asterisk: PTFE porous membrane; black asterisk: location of the polyester mesh. Scale bars: 100 µm. F) Representative single-cell response of the YC3.6$_{cyto}$ calcium sensor to glucose (16.7×10^{-3} M) stimulation upon cells retrieved from capsules, implanted eight weeks in mice. The ratiometric signal (R) was normalized to basal (R_0). The effects of diazoxide (100×10^{-6} M) and KCl (30×10^{-3} M) are also shown. The experiment was repeated eight times.

The pronounced effect on glucose homeostasis demonstrates that the encapsulated INS-1E cells contribute strongly to total insulin secretion in the mice. To verify that encapsulated INS-1E cells were solely responsible for the accelerated glucose clearance, we surgically removed the capsule from two mice (capsules originally loaded with 3 million cells) after seven weeks of implantation. After implant removal, glucose clearance was comparable to control mice, confirming that insulin secretion from encapsulated cells was responsible for the observed enhanced glucose clearance (Figure 4C). These results demonstrate that encapsulated cells contributed to glucose regulation in mice and therefore INS-1E cells are viable and functional when encapsulated and implanted in vivo. Both the 1 and 3 million cells conditions were effective in promoting successful growth, although devices loaded with 1 million cells took longer to reach the required biomass to significantly contribute to glycaemia regulation.

For each of the cell loading conditions, devices were explanted at two, four, and seven or eight weeks to measure the fluorescence emitted by encapsulated cells. High levels of fluorescence was measured, confirming that encapsulated INS-1E cells were viable and stably expressed the calcium sensor in vivo (Figure 4D). The fluorescence level was comparable to fluorescence measured from capsules cultured in stirred medium conditions, indicating good oxygenation and nutrient supply in vivo. These results were confirmed by histological analysis revealing a highly dense mass of viable cells close to the porous membranes (Figure 4E). The explanted INS-1E cells responded to glucose by strongly increasing calcium signaling in response to glucose (Figure 4F) showing that they retained their ability to undergo normal metabolism-secretion coupling. Diazoxide terminated glucose-dependent calcium signaling and plasma membrane depolarization with KCl induced massive calcium influx, confirming beta-cell like behavior of INS-1E cells derived from in vivo encapsulation experiments. In addition, we noticed complete synchronization of single-cell calcium transients from cell clusters (Figure 4F). This extent of synchronization is not observed when monolayers of INS-1E cells are cultured in vitro (data not shown[22]). These results demonstrate that INS-1E cells expressing the calcium sensor YC3.6$_{cyto}$ are viable and functional in vivo, and stably maintain a high

level of fluorescence, which makes them a suitable model for the proposed in vivo cell-based biosensor.

3. Discussion

Recently, there has been growing interest in developing cell-based biosensors platform giving insight into cell and tissue function. Various genetic probes based on FRET technology have been developed, triggering the development of optical sensors to monitor intracellular parameters.[11,23] Here, we have generated a stable clone of INS-1E pancreatic beta-cell expressing the YC3.6$_{cyto}$ calcium sensor, which has been extensively tested in vitro and in vivo. We have demonstrated that this stable cell line can be encapsulated and implanted in vivo for an extended period of time, and therefore serve as an essential building block of an in vivo cell-based biosensor.

A 3D structure is essential for cell encapsulation in order for the cells to growth in a tissue-like organization. We demonstrated that INS-1E cells can be cultured in suspension to form aggregates of stable size and shape. The size of the aggregates can be tailored for specific requirements by controlling the speed of the orbital shaker. This property of INS-1E cells could also be used to replace adherent culture when performing functional tests, since aggregates increase cell–cell interaction which better mimics the in vivo conditions. In addition, aggregates were effective in providing a 3D structure favoring cell growth and function within the encapsulation devices. Excellent glucose-stimulated insulin secretion ratios were observed from encapsulated cells, suggesting that the 3D environment of the capsule was favoring insulin secretion from INS-1E cells.

The different clones expressing the calcium sensor showed different outcome when encapsulated in vitro. These differences are explained by the heterogeneity of INS-1E cells and the development method of these clones. The clones were selected by FACS sorting and expanded from single cells originating from a heterogeneous cell population. Differences between clones were therefore expected, which led us to test and compare the function and encapsulation capabilities of three clones. Out of the three clones extensively tested, one showed particularly good survival and insulin secretion function when encapsulated in vitro for an extended period of time. The spontaneous cluster formation in adherent culture indicates increased cell–cell interactions for this clone. This property of the INS-1E cell clone may explain better survival and function in the capsule. These differences observed in vitro, which seems to be linked to different phenotypes originating from the same cell line, emphasize the importance of performing functional in vitro testing when developing such a clone, in order to maximize the chance of success in vivo.

Successful in vivo encapsulation of cells depends on many parameters including initial cell density, semipermeable membrane porosity, and 3D microenvironment.[9] In particular, cell density has been shown to be a critical parameter for the successfully engraftment of implanted cells using a macroencapsulation system.[8] Here, we show that two different cell densities enable good survival and function of encapsulated INS-1E-YC3.6$_{cyto}$ cells in vivo. This demonstrates the robustness of INS-1E-YC3.6$_{cyto}$ cell encapsulation and the capability of these cells to adapt to reduced oxygen and nutrient environment conditions. When the lower cell density (1 million cells at the start of device loading) was used, the cells were able to expand quite rapidly inside the device. Such a low density should be favored to avoid massive cell death after implantation of the capsule, which could hinder proper cell growth for long term implantation.[8] In addition to good survival, the maintenance of a high fluorescence level in vivo is important to allow the detection of the signal with a photodiode-based implanted optical sensor. The fluorescence intensity of the cells is strongly dependent upon oxygen and nutrient availability when encapsulated in vitro. This was concluded from our observation that fluorescence levels inside capsules maintained in vitro rapidly increases in stirred medium conditions. Strong YC3.6 fluorescence was also observed in explanted devices two, four, and eight weeks after transplantation, suggesting a good oxygen and nutrient supply in vivo. These findings are promising for the use of this stable cell line in the proposed in vivo biosensor.

The synchronization of calcium response observed after in vivo encapsulation illustrates well the potential effects generated by the in vivo environment on implanted cells. This synchronization of calcium signaling in INS-1E cells probably indicate improved intercellular connectivity and communication, which has been shown to influence insulin secretion,[24] with beneficial effects on beta-cell activation in vivo. The use of this cell line for the study of beta-cell activation in vivo requires the development of an implantable optical sensor based on small size optical elements with good sensitivity controlled by an electronic system. Ultrasmall light-emitting devices have recently been demonstrated in vivo, in particular for optogenetic applications, where an implanted photodiode control trans-gene expression.[10,25] Cell-based biosensors, which have been mostly applied to bacterial systems and toxicity applications up to now, are expected to become a major research topic with potential for broad application in biomedical research and medicine.[23]

4. Conclusion

In order to create advanced tools for biomedical research, we report the development of a pancreatic beta-cell line expressing a calcium sensor for the study of beta-cell activation in vivo. Following optimization of aggregation and encapsulation in vitro, implantation in mice demonstrated that encapsulated INS-1E cells expressing the YC3.6$_{cyto}$ calcium sensor are viable and functional in vivo. We have developed the cellular part of an in vivo biosensor, which has the potential to advance the study of metabolic diseases by allowing in vivo monitoring of beta-cell function and its relationship to diet, exercise, and aging.

5. Experimental Section

Reagents: Chemicals were from Sigma, Invitrogen, or VWR unless otherwise indicated. The YC3.6$_{cyto}$pcDNA3 construct[2] was kindly provided by Dr. A. Miyawaki (Riken Brain Science Institute, Wako, Japan).

Cell Culture: INS-1E cells were cultured at 37 °C in a humidified atmosphere (5% CO_2) in RPMI 1640 medium (Invitrogen) containing

11×10^{-3} M glucose, supplemented with 10×10^{-3} M Hepes (pH 7.3), 10% (v/v) heat-inactivated fetal calf serum (Brunschwig AG), 1×10^{-3} M sodium pyruvate, 50×10^{-6} M β-mercaptoethanol, 50 µg mL^{-1} penicillin, and 100 µg mL^{-1} streptomycin.

Aggregates Viability: The viability of INS-1E cells in aggregates was determined using the Live/Dead Viability/Cytotoxicity Assay Kit (Molecular Probe, Carlsbad, USA). Aggregates were incubated in Krebs–Ringer bicarbonate Hepes (KRBH) containing fluorescent dyes at the concentrations of 2×10^{-3} M Calcein-AM and 12×10^{-3} M ethidium homodimer-1 for 45 min. Aggregates were washed with KRBH and visualized with a Zeiss Axioimager upright microscope.

Encapsulation Device: Encapsulation of INS-1E and INS-1E-YC3.6$_{cyto}$ cells were investigated using a flat sheet encapsulation device based on a polymeric frame technology described in ref. [8]. Basically, a medical grade polypropylene frame holds two parallel porous membranes creating the encapsulation compartment, and two outer reinforcement polyester meshes. Hydrophilized PTFE (polytetrafluoroethylene) membranes with 0.4 µm nominal pore size (Millipore) were used as porous material. These membranes fully confine cells within the encapsulation device while allowing diffusion of all molecules. They restrict the access of immune cells to encapsulated cells while allowing the transport of antibodies and complement components, which make cells fully immune-protected in allogenic but not in xenogenic transplantations. An external port integrated in the polymeric frame, which was subsequently cut and sealed, was used to load the cell suspension into the encapsulated device.

In Vitro Insulin Secretion from Encapsulated Cells: Insulin secretion experiments were performed in KRBH buffer containing 140×10^{-3} M NaCl, 3.6×10^{-3} M KCl, 0.5×10^{-3} M NaH_2PO_4, 0.5×10^{-3} M $MgSO_4$, 1.5×10^{-3} M $CaCl_2$, 10×10^{-3} M Hepes, and 5×10^{-3} M $NaHCO_3$ (pH 7.4). Encapsulation devices were placed in 6-well culture plates in KRBH buffer, containing 2.5×10^{-3} or 16.7×10^{-3} M glucose, and 0.1% BSA (bovine serum albumin). The encapsulation devices were preincubated for 60 min at 2.5×10^{-3} M glucose, then incubated in basal glucose (2.5×10^{-3} M) for 60 min, and finally stimulated with high glucose (16.7×10^{-3} M) for 60 min. During the experiment, the culture plates were placed on an orbital shaker to ensure that insulin secreted by encapsulated cells was mixed with the culture medium. Supernatants were saved after basal and stimulated incubation, and insulin was measured using an enzyme immunoassay kit (SPI bio, Massy, France).

Generation of INS-1E-YC3.6$_{cyto}$ Clonal Cell Lines: INS-1E cells were plated on polyornithine-treated 10 cm diameter dishes and transfected with the expression vector carrying the YC3.6$_{cyto}$ sensor [Nagai, 2004] using DharmaFECT transfection reagent (Thermo Scientific). Stable transformants were selected using a two-steps selection procedure with G418 (300 µg mL^{-1}). After 4 d selection, high-fluorescent cells were sorted by FACS at 488 nm emission. Selected cells were grown for additional 20 d in the selection medium. Cells were then sorted by FACS and single-cell plated on 96-well plates. The single-colony YC3.6$_{cyto}$ signals were detected by fluorescence.

Single Cell Imaging of Cytosolic Ca^{2+} Signals: INS-1E cells stably expressing the genetically encoded cameleon sensors YC3.6$_{cyto}$ were plated on polyornithine-treated 35 mm diameter glass-bottom dishes (MatTek). One day after, cells were washed four times and experiments were performed at 37 °C in KRBH. Glass coverslips were inserted in a thermostatic chamber (Life Imaging Services). The cells were preincubated for 15 min in KRBH basal (2.5×10^{-3} M) glucose before recording. Cells were imaged on a DMI6000 B inverted fluorescence microscope using a HCX PL APO 63 × /1.40–0.60 NA oil immersion objective (Leica Microsystems) and an Evolve 512 back-illuminated CCD (charge-coupled device) with 16×16 µm pixels camera (Photometrics, Tucson, AZ), as previously described.[26] Cells were excited at 430 nm through a BP436/20 filter. The two emission images were acquired with BP480/40 and BP535/30 emission filters. Fluorescence ratios were calculated in MetaFluor 7.0 (Meta Imaging Series) and analyzed in Excel (Microsoft). Images were taken every 2 s.

Device Loading and Implantation: The aggregates were allowed to settle by gravity. 10–30 µL of cell aggregate slurry (representing 1–3 million cells) were suspended in 0.9 mL of culture medium. A 1 mL syringe was used to load the cell aggregate suspension into the encapsulation device, which was filled beforehand with PBS (phosphate-buffered saline). The loading port was cut and the device sealed using ultraviolet curing adhesive (Loctite 3311). The devices were maintained in culture medium in an incubator until the implantation, typically occurring the next day.

Since the encapsulation device was not fully immune-protective for xenogenic transplantation, immune-compromised SCID/beige mice were used. For implantation, mice were anesthetized by inhalation of 3% isoflurane. An incision was made caudal to the shoulder blade and the device was implanted in the dorsal subcutaneous space. Wounds clips were used to close the cut. After surgery, animals received 2 mg mL^{-1} of paracetamol in drinking water for 3 d. The animal experiment was carried out in accordance with the Swiss regulation on animal experimentation and the European Council directive (86/609/EEC) for the care and use of laboratory animals.

Static Glucose-Stimulated Insulin Secretion in Mice: The insulin secretion function of encapsulated INS-1E-YC3.6$_{cyto}$ cells was evaluated by static glucose-stimulated insulin secretion. Following overnight fasting, animals received an intraperitoneal injection of a 20% glucose solution dosed at 2.0 g kg^{-1} body weight. Blood samples were collected before and following the glucose injection at 15, 30, and 60 min. The effect of the implant on glycaemia regulation was determined by measuring the glucose clearance from the body after the intraperitoneal injection. Glucose concentration was determined from blood samples using a glucometer with test strips (Accu-check).

Histology: Encapsulation devices were fixed in 4% paraformaldehyde overnight at 4 °C, dehydrated, and processed for paraffin embedding. Samples were sectioned at a thickness of 5 µm and stained with hematoxylin and eosin. Images were acquired with a bright-field microscope (Leica) with a 10× objective.

Acknowledgements

The authors gratefully acknowledge Roy Combe and Arnaud Bichat (EPFL Center of Phenogenomics) for animal experimentation. The authors thank Prof. A. Miyawaki (Riken Brain Science Institute) for sharing YC3.6pcDNA3 construct.

Received: August 4, 2016
Revised: November 4, 2016
Published online:

[1] J. Zhang, R. E. Campbell, A. Y. Ting, R. Y. Tsien, *Nat. Rev. Mol. Cell Biol.* **2002**, *3*, 906.
[2] T. Nagai, S. Yamada, T. Tominaga, M. Ichikawa, A. Miyawaki, *Proc. Natl. Acad. Sci. USA* **2004**, *101*, 10554.
[3] a) H. Takanaga, B. Chaudhuri, W. B. Frommer, *Biochim. Biophys. Acta* **2008**, *1778*, 1091; b) H. Imamura, K. P. Nhat, H. Togawa, K. Saito, R. Iino, Y. Kato-Yamada, T. Nagai, H. Noji, *Proc. Natl. Acad. Sci. USA* **2009**, *106*, 15651.
[4] a) D. Poburko, J. Santo-Domingo, N. Demaurex, *J. Biol. Chem.* **2011**, *286*, 11672; b) G. T. Hanson, R. Aggeler, D. Oglesbee, M. Cannon, R. A. Capaldi, R. Y. Tsien, S. J. Remington, *J. Biol. Chem.* **2004**, *279*, 13044.
[5] C. H. Contag, M. H. Bachmann, *Annu. Rev. Biomed. Eng.* **2002**, *4*, 235.
[6] F. Leblond, S. C. Davis, P. A. Valdes, B. W. Pogue, *J. Photochem. Photobiol., B* **2010**, *98*, 77.
[7] J. D. Newman, A. P. Turner, *Biosens. Bioelectron.* **2005**, *20*, 2435.
[8] A. Lathuiliere, S. Cosson, M. P. Lutolf, B. L. Schneider, P. Aebischer, *Biomaterials* **2014**, *35*, 779.

[9] H. Uludag, P. De Vos, P. A. Tresco, *Adv. Drug Delivery Rev.* **2000**, *42*, 29.
[10] T. I. Kim, J. G. McCall, Y. H. Jung, X. Huang, E. R. Siuda, Y. Li, J. Song, Y. M. Song, H. A. Pao, R. H. Kim, C. Lu, S. D. Lee, I. S. Song, G. Shin, R. Al-Hasani, S. Kim, M. P. Tan, Y. Huang, F. G. Omenetto, J. A. Rogers, M. R. Bruchas, *Science* **2013**, *340*, 211.
[11] M. Choi, J. W. Choi, S. Kim, S. Nizamoglu, S. K. Hahn, S. H. Yun, *Nat. Photonics* **2013**, *7*, 987.
[12] M. J. Berridge, P. Lipp, M. D. Bootman, *Nat. Rev. Mol. Cell Biol.* **2000**, *1*, 11.
[13] a) A. Wiederkehr, C. B. Wollheim, *Cell Calcium* **2008**, *44*, 64; b) A. Wiederkehr, C. B. Wollheim, *Mol. Cell Endocrinol.* **2012**, *353*, 128.
[14] a) M. Whitaker, *Methods Cell Biol.* **2010**, *99*, 153; b) A. E. Palmer, Y. Qin, J. G. Park, J. E. McCombs, *Trends Biotechnol.* **2011**, *29*, 144.
[15] N. Demaurex, *Cell Calcium* **2005**, *38*, 213.
[16] A. E. Palmer, M. Giacomello, T. Kortemme, S. A. Hires, V. Lev-Ram, D. Baker, R. Y. Tsien, *Chem. Biol.* **2006**, *13*, 521.
[17] U. De Marchi, C. Castelbou, N. Demaurex, *J. Biol. Chem.* **2011**, *286*, 32533.
[18] A. D. Agulnick, D. M. Ambruzs, M. A. Moorman, A. Bhoumik, R. M. Cesario, J. K. Payne, J. R. Kelly, C. Haakmeester, R. Srijemac, A. Z. Wilson, J. Kerr, M. A. Frazier, E. J. Kroon, K. A. D'Amour, *Stem Cells Transl. Med.* **2015**, *4*, 1214.
[19] a) D. W. Hopcroft, D. R. Mason, R. S. Scott, *Endocrinology* **1985**, *117*, 2073; b) F. Jaques, H. Jousset, A. Tomas, A. L. Prost, C. B. Wollheim, J. C. Irminger, N. Demaurex, P. A. Halban, *Endocrinology* **2008**, *149*, 2494.
[20] A. Merglen, S. Theander, B. Rubi, G. Chaffard, C. B. Wollheim, P. Maechler, *Endocrinology* **2004**, *145*, 667.
[21] J. Jo, M. Y. Choi, D. S. Koh, *Biophys. J.* **2007**, *93*, 2655.
[22] A. Wiederkehr, G. Szanda, D. Akhmedov, C. Mataki, C. W. Heizmann, K. Schoonjans, T. Pozzan, A. Spat, C. B. Wollheim, *Cell Metab.* **2011**, *13*, 601.
[23] Q. Liu, C. Wu, H. Cai, N. Hu, J. Zhou, P. Wang, *Chem. Rev.* **2014**, *114*, 6423.
[24] a) I. Konstantinova, G. Nikolova, M. Ohara-Imaizumi, P. Meda, T. Kucera, K. Zarbalis, W. Wurst, S. Nagamatsu, E. Lammert, *Cell* **2007**, *129*, 359; b) M. J. Luther, A. Hauge-Evans, K. L. Souza, A. Jorns, S. Lenzen, S. J. Persaud, P. M. Jones, *Biochem. Biophys. Res. Commun.* **2006**, *343*, 99; c) M. A. Ravier, M. Guldenagel, A. Charollais, A. Gjinovci, D. Caille, G. Sohl, C. B. Wollheim, K. Willecke, J. C. Henquin, P. Meda, *Diabetes* **2005**, *54*, 1798.
[25] J. W. Jeong, J. G. McCall, G. Shin, Y. Zhang, R. Al-Hasani, M. Kim, S. Li, J. Y. Sim, K. I. Jang, Y. Shi, D. Y. Hong, Y. Liu, G. P. Schmitz, L. Xia, Z. He, P. Gamble, W. Z. Ray, Y. Huang, M. R. Bruchas, J. A. Rogers, *Cell* **2015**, *162*, 662.
[26] U. De Marchi, J. Thevenet, A. Hermant, E. Dioum, A. Wiederkehr, *J. Biol. Chem.* **2014**, *289*, 9182.